International Journal of Artifical And Neural Networks – IJAINN 2018
Copyright © Institute of Research Engineers and Doctors , SEEK Digital Library
Volume 8 : Issue 1- [ISSN : 2250-3749] - Publication Date: 28 December, 2018

Numerical Prediction on Two Phase Flow through an 180˚ pipe bend

B B Nayak, D Chatterjee and A N Mullick

***Abstract*— A three dimensional numerical study of flow characterized of fly ash-water slurry in a horizontal 180˚ pipe bend having radius ratio of 5.6 is described in this paper. The flow constitutes the fly ash particles of size 13 µm in water at velocities ranging between 1.0-5.0 m/s and particle concentrations ranging between 10-50% by volume for each velocity of flow. The numerical simulation is carried out by deploying the Eulerian Multiphase Model of CFD code in ANSYS Fluent code. The results illustrate that the overall pressure drop is 62% in the pipe bend at all particle velocities and concentrations. The velocity and concentration distributions at various positions (0˚, 90˚ and 180˚) of the bend were illustrated.**

Keywords—*U-bend, two phase flow, numerical simulation. Eulerian Multiphase approach*

I. Introduction

The 180˚pipe bends are integral part of the piping system used for transportation and in heat exchangers in almost all Industrial applications. For all high Reynolds Number flow a secondary flow originates in the bend portion due to the imbalance in centrifugal force in the curvature of bend and which in turn leads to the excess pressure loss across the curved portion of the pipes. In the present work, pressure drop is predicted in a horizontal 180˚ pipe bends for the flow of water-fly ash slurry. Azzola *et al.* [1] used the Laser Doppler Velocimetry technique to measure the longitudinal and circumferential velocity components for developing turbulent flow in 180˚ pipe bend. They observed the reversal of secondary flow in circumferential velocity profile and it is independent of Reynolds Number. Jayanti et. al. [2] studied the numerical simulation of gas particle motion in 90° and 180° circular cross section pipe bends and concluded that the secondary flow induced in the gas phase due to the curvature effect. Clarke and Finn [3] did the numerical simulation of laminar flow of potassium formate through heat exchanger U-bends and observed an enhancement of heat transfer at downstream of the bend. Al-Yaari and Abu-Sharkh [4] numerically simulated oil-water two-phase flow in 180˚ bends using Eulerian-Eulerian approach and observed as the bend to pipe radius ratio increases, the tendency of separation of oil water system decreases. Muzumder [5] performed CFD simulation of dilute gas-solid flow through a U-Bend to study the dynamic behavior of the entrained solid particles in the flow and observed that the liquid and the gas flow rates, gravity and centrifugal forces have a strong effect on the flow behavior. Pietrzak and Witczak [6] performed experimental research on multiphase flow in 180˚ U-bends using three flowing media, namely, air, water and oil obtained the flow pattern and pressure drop correlations for horizontal, upward and downward flows. . Daneshfaraz [7] study numerically the velocity profile and pressure distribution on 3-D bends with different diversion angles of 90^0, 135^0, 180^0 and Reynolds number range of 100 to 1900 using CFD. He concluded that by increasing the section angle, the velocity profile and the pressure distribution incline to the outer wall and maximum deviation from inlet velocity profile occurs at 45° section angle. The maximum velocity occurs at 0.7 to 0.9 of the pipe diameter from linear wall and the maximum pressure loss occurs at angle between 22.5° and 45° with increasing Reynolds Number. Cvetkovski *et al.* [8] carried out numerical simulation of flow in U-bend pipes used in ground source and surface heat pumps for heating and cooling purposes and observed that at low turbulence, the Dean Number has a significant effect on the heat transfer in the curved section. They also concluded that the heat transfer at the curved section has of the pipe has more significant effect on Dean Number than the Reynolds Number

So far, the study of flow behavior of two-phase fly ash-water slurry flow in 180° bends at high concentrations is limited. The present study is a numerical prediction of flow characteristics of the two-phase flow in an 180˚ horizontal pipe bend using fly ash of particles diameter 13 µm suspended in water at high velocities and concentrations factor ranging from 10 to 50%.

II. Physical problem

The horizontal 180˚ bend pipe of length about L = 11m with an inner diameter of D = 0.053 m having radius ratios (R/r) of 5.6 is chosen as the slurry transportation device as shown in Figure 1.

A. *Governing Equation*

Continuity equations for the solid and liquid phases

$$\nabla \cdot (\alpha_s \rho_s \vec{v}_s) = 0 \qquad \nabla \cdot (\alpha_f \rho_f \vec{v}_f) = 0$$

Momentum equations for the solid and liquid phases

$$\nabla.(\alpha_s \rho_s \vec{v}_s \vec{v}_s) = -\alpha_s \nabla P - \nabla P_s + \nabla \bar{\bar{\tau}}_s + \alpha_s \rho_f \vec{g} + K_{fs}(\vec{v}_f - \vec{v}_s) + C_{vm}\alpha_s \rho_f (\vec{v}_f.\nabla \vec{v}_f - \vec{v}_s.\nabla \vec{v}_s) + C_L \alpha_s \rho_f (\vec{v}_s - \vec{v}_f) x (\nabla x \vec{v}_f)$$

B B Nayak and A N Mullick
National Institute of Technology Durgapur
India
D Chatterjee
CMERI, India

where α_s , ρ_s , v_s and α_f , ρ_f , v_f are volume fraction, density and velocity of solid and liquid, respectively. ∇P_s and ∇P are the collisional solid stress in solid phase due to particle collisions and pressure shared by all phase, $\bar{\bar{\tau}}_s$ and $\bar{\bar{\tau}}_f$ are the viscous stress tensors for solid and fluid, respectively.

$$\bar{\bar{\tau}}_s = \alpha_s \mu_s (\nabla \vec{v}_s + \nabla \vec{v}_s^{tr}) - \alpha_s (\lambda_s - \frac{2}{3}\mu_s) \nabla \cdot \vec{v}_s \bar{\bar{I}}$$

$$\bar{\bar{\tau}}_f = \alpha_f \mu_f (\nabla \vec{v}_f + \vec{v}_f^{tr})$$

The superscript 'tr' over the velocity vector indicates transpose. $\bar{\bar{I}}$ is the identity sensor.

λ_s is the bulk viscosity of the solids as given by Lun et. al. [9]

$$\lambda_s = \frac{4}{3}\alpha_s \rho_s d_s g_{o,ss} (1+e_{ss}) \left(\frac{\theta_s}{\pi}\right)^{\frac{1}{2}}$$

$g_{o,ss}$ is the radial distribution function, which is interpreted as the probability of particle touching with another particle given by Gidaspow *et. al.* [10].

$$g_{o,ss} = \left[1 - \left(\frac{\alpha_s}{\alpha_{s,\max}}\right)^{\frac{1}{3}}\right]^{-1}$$

$\alpha_{s,\max}$ is the static settled concentration taken as 0.63 in the present study as the ash particles are modeled as mono-dispersed spheres. θ_s is the granular temperature which is proportional to the kinetic energy of the fluctuating particle motion, e_{ss} is the restitution coefficient, taken as 0.9 for fly ash particles.

B. *Metodology*

The commercial CFD package ANSYS Fluent [11] is use for performing the numerical simulation. A second order upwind scheme is applied for the discretization of the momentum equations. Turbulent kinetic energy, dissipation rate of turbulent kinetic energy equations and volume fraction equations are discretized using the first order discretization scheme. The pressure based numerical scheme, which solves the discretized governing equations sequentially, is selected. PCSIMPLE algorithm is selected as pressure-velocity coupling scheme. The convergence criterion for the calculated variables (mass, velocity components, turbulent kinetic energy, turbulent kinetic energy dissipation rate, volume fraction and temperature) is set as 10^{-3}. The under-relaxation factors for momentum are kept in the range of 0.5-0.7, pressure was chosen in the range of 0.2-0.3, while the turbulent kinetic energy and its dissipation rate are in the range of 0.6-0.8.

A structured grid system with hexagonal elements consisting of 697566 cells for the bend of radius ratio 5.6 is used for discretization of the entire computational domains as shown in Figure 2. A grid independence study is also conducted by choosing another two sets of grids having cells 465044 and 1046349 for the geometry. As medium and largest cells have lower variation in pressure drops, hence medium cell meshes are considered in the study.

III. Result and Discussion

A comparison of the present numerical results in terms of normalized pressure drop is made with the experimental results of Kaushal et al. [12] along the pipe length at particle velocity of 3.56 m/s and concentration of 16.28%. The results obtained are in very good agreement with the experimental data [12] as shown in Figure.3.

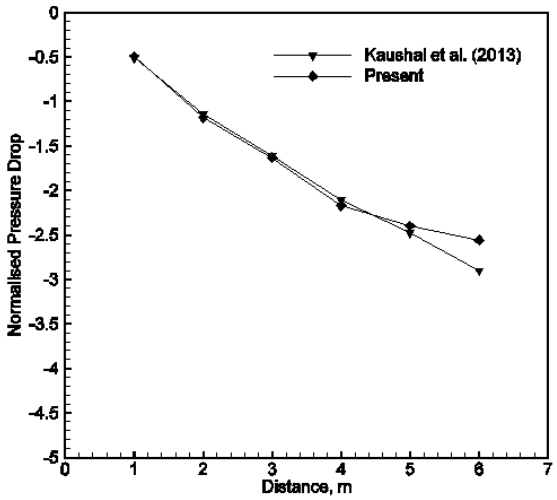

Fig 3 Comparison of results with the experimental data [12]

A. *Pressure drop at bend*

Figure 4 shows the variations of pressure drop at different particle velocities and concentrations in the 180˚ pipe bend. At lower velocities, increasing the particle concentration the increase of pressure drops are 35%, 52% and 73%; a rise up to 85% as observed at higher velocities and concentration. The pressure drop increases at higher velocities because of more interaction of the particles due to turbulence. The pressure drop increases at higher concentrations due to steep increase in the viscosities of the slurry. The two phase pressure drop in the bend is affected not only by the secondary flow effects as observed in single phase flows, but also by the separation of phases due to centrifugal forces which concentrates the particles towards the concave (outside) portion, while the water flows towards the convex (inside) portion. This increases the relative motion between the phases and pressure drop. Due to flow separation at the inner side of the bend near to the entry and exit of the 180˚ bend two mixing layers are formed and energy dissipation in eddies in these layers causes the pressure drop.˃

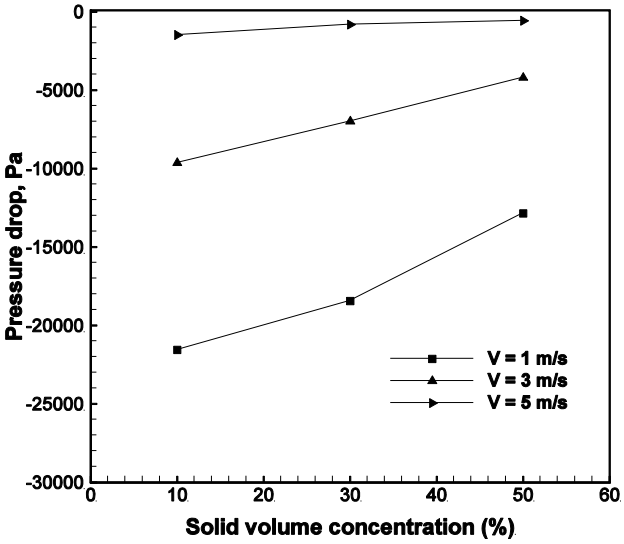

Figure 4 Variation of slurry pressure drop at different particle velocities and concentrations

B. *Velocity Distribution at bend*

The velocity distribution contours at bend inlet (0˚), 90˚and outlet (180˚) for a velocity of 1 m/s and concentrations of 10%, 30% and 50% for the slurry flow in the bend are shown in Figure 5. When slurry enters to the U-bend a pressure gradient develops due to the development of higher pressure towards the outside wall of the bend and lower pressure towards the inside wall of the bend. It has been observed that the higher velocity zone remains in the central core of the pipe cross-section at the bend inlet. The secondary flow, which starts from 45˚ and increases from 90˚ to 180˚, traps the particles to move further up along the pipe wall. At the bend outlet, velocity at the outer wall becomes more due to the action of the centrifugal forces.

C. *Concentration distribution at bend*

The concentration distribution contours at bend inlet, center and bend exit for the velocity of 1 m/s and concentrations of 10%, 30% and 50% are as shown in Figure 6. . In the bend portion, the maximum concentration is found at the outer side of the bend inlet. The particles move towards the outer side of the wall due to centrifugal force and curvature effect from 45˚ angle of the bend. The secondary flow which starts from 45˚ and increases up to 180˚ moves the particles towards the inner side of the wall towards the center. It is due to the fact that the secondary flow drives the particles at the core of the pipe forcing towards the outer side of the wall.

IV. Conclusions

A three-dimensional model is developed using ANSYS FLUENT software to investigate the flow behavior of fly ash-water slurry in a 180˚ return bend. The simulation is performed considering the mean slurry velocity ranging from 1-5 m/s and the volume fraction of the solid ranging from 10-50% with fly ash particle sizes of 13 µm in water. The pressure drop is investigated for various particle volume concentration and velocities. The following conclusions can be made based on the numerical study:

1. The Euler model provides a good numerical prediction for the pressure gradients in the liquid-solid slurry flow and is in good agreement with the experimental data [12].
2. The pressure drop in 180° return bend is observed to increase in the mean inflow velocity and the particle volume concentration.
3. The pressure drop in 180˚ return bends increases with increase in the velocity and particle volume concentration. Its value changes from 35% to 85% for the change of concentration from 10% to 50% for the same velocity.
4. At the U bend portion, the secondary flow drives the particles at the core of the pipe forcing towards the outer side of the wall.

References

[1] Azzola J, Humphrey J A C, Lacovides H and Launder B E 1986 Developing turbulent flow in a U-bend of circular cross-section: Measurement and computation, J. Fluids Eng. 108 214-21.

[2] Jayanti S., Wang M. J. and Mayinger F., 1993 Gas particle flow through bends, IMechE, C461, 24, 161-166.

[3] Clarke R. and Finn D. P., 2008, Numerical Investigation of the Influenceof Heat Exchanger U-bends on temperature profile and heat transfer of secondary working fluids, 5th European Thermal Science Conference, The Netherlands, 1-8.

[4] Al-Yaari M A and Abu-Sharkh B F 2011, CFD prediction of oil-water phase separation in 180˚ bend, Asian Trans. Eng. 1 63-67.

[5] Mazumder Q H 2012, Effect of liquid and gas velocities on magnitude and location of maximum erosion in U-bend, Open J. Fluid Dyn. 2 29-34.

[6] Pietrzak M and Witczak S 2013 Multiphase flow mixture in 180˚ pipe bends, Chem. Process Eng. 34 227-39.

[7] Daneshfaraz R 2013 3-D investigation of velocity profile and pressure distribution in bends with different diversion angle, J. Civil Eng. Sci. 2 234-40.

[8] Cvetkovski C G, Reitsma S, Bolisetti T and Ting D S K 2015 Heat transfer in a U-Bend pipe: Dean number versus Reynolds number, Sust. Ener. Tech. Assess. 11 148-58.

[9] Lun C K K, Savage S B, Jeffrey D J and Chepurniy N 1984 Kinetic theories for granular flow: inelastic particles in Couette flow and slightly inelastic particles in a general flow field. J. Fluid Mech. 140 223-56.

[10] Gidaspow D and Lu H 1998 A comparison of gas-solid and liquid-solid fluidization using kinetic theory and statistical mechanics. In: Fan L.S., Knowlton , T.M (Eds.), Fluidization IX. Engineering Foundation, New York 661-68.

[11] ANSYS Fluent, ver. 14.0, 2011 Theory Guide, Ansys Inc., USA.

[12] Kaushal D R, Kumar A, Tomita Y, Kuchii S and Tsukamoto H 2013 Flow of Mono-Dispersed Particles through Horizontal Bend, Int. J. Multiphase Flow. 52 71-91.

International Journal of Artifical And Neural Networks – IJAINN 2018
Copyright © Institute of Research Engineers and Doctors , SEEK Digital Library
Volume 8 : Issue 1- [ISSN : 2250-3749] - Publication Date: 28 December, 2018

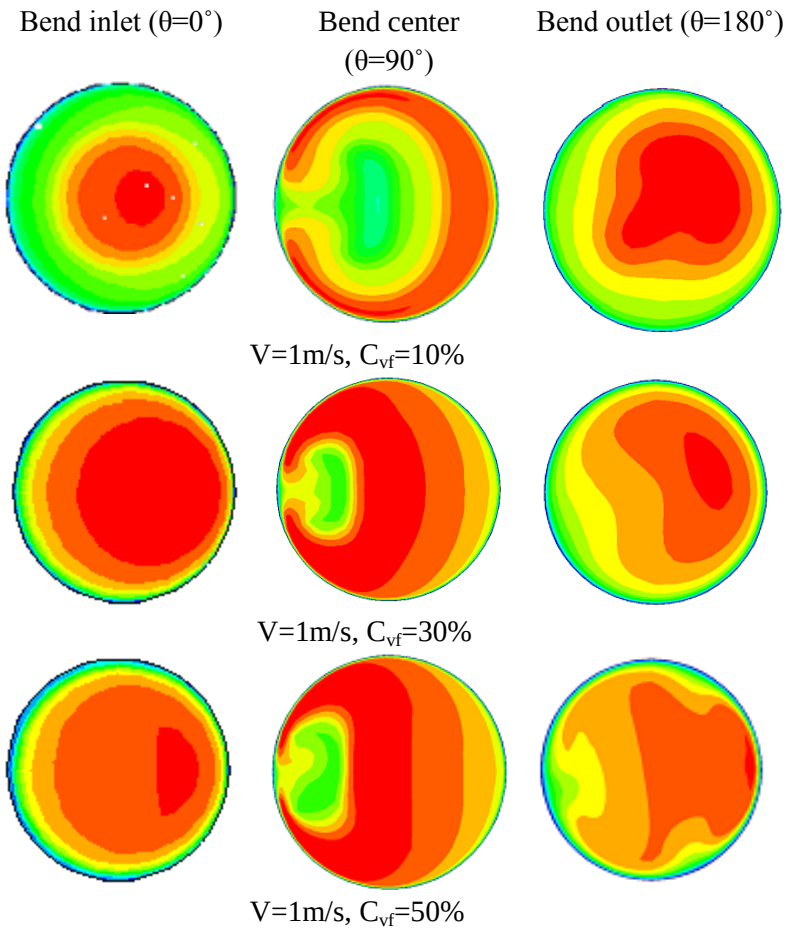

Figure 5 Distribution of velocity for different velocities and concentrations of the particles.

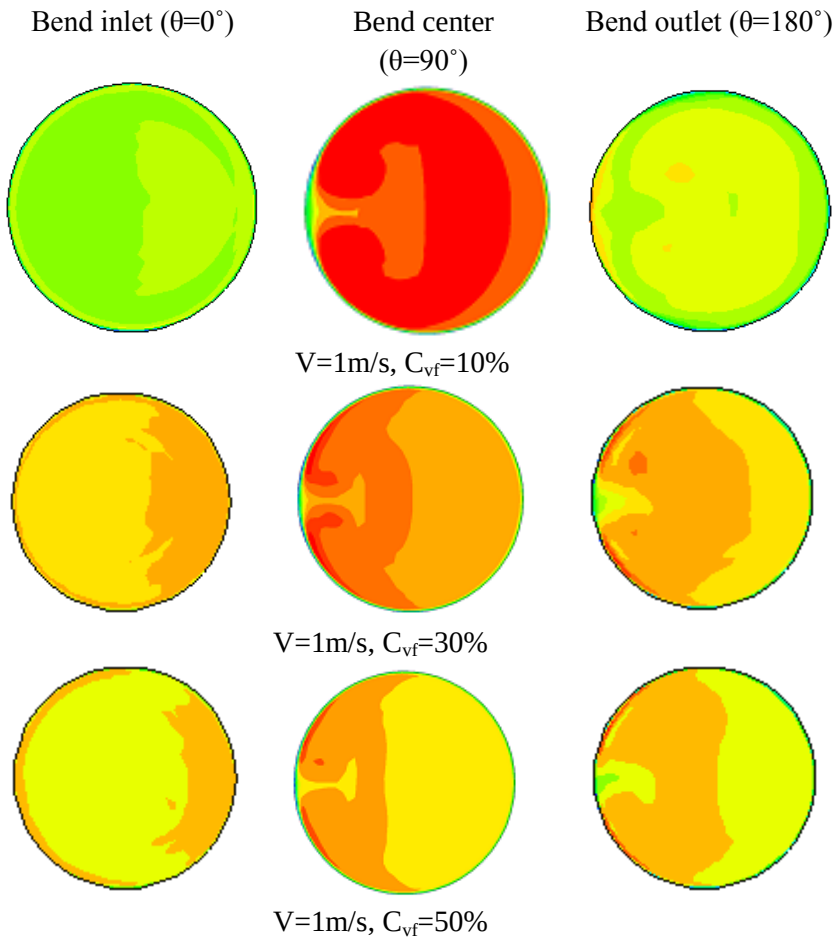

Figure 6 Distribution of velocity for different velocities and particle concentrations